Cyclodextrin-Based Pseudopolyrotaxanes as Templates for the Generation of Porous Silica Materials

ARTICLE *in* CHEMISTRY OF MATERIALS · AUGUST 2002

Impact Factor: 8.35 · DOI: 10.1021/cm0113088 · Source: OAI

Cyclodextrin-Based Pseudopolyrotaxanes as Templates for the Generation of Porous Silica Materials

Bao-Hang Han* and Markus Antonietti

Max Planck Institute of Colloids and Interfaces, 14424 Potsdam, Germany

Received December 17, 2001. Revised Manuscript Received May 14, 2002

The in situ formed supramolecular assemblies of cyclodextrins with nonionic surfactants, poly(ethylene glycol), poly(propylene glycol), and block copolymer, so-called pseudopolyrotaxanes, were used as porogens for the generation of porous silica materials. The resulting structures are characterized with nitrogen sorption experiments, transmission electron microscopy, and small-angle X-ray scattering. It was shown that the pore structure replicates the structure of the original supramolecular template, i.e., at pH 2.0, the cyclodextrins are threaded by the polymer, and a short tubelike morphology of the pores is found. At higher pH values, the aggregation of the pseudopolyrotaxanes toward bundle domains leads to larger pores.

Introduction

Starting from the invention of the ordered mesoporous silicas, such as M41S introduced by the Mobil group (Beck, Vartuli, and Kresge et al.) in 1992,[1] synthesis of porous inorganics by organic porogens has become one of the most active fields in modern materials chemistry. Meanwhile, it is safe to state that a whole "construction kit" is available to tailor-make porous materials on a recombinatorial base.[2−8]

Whereas the classical M41S synthesis is a synthesis in dilute solution where the product precipitates as a micron-scale powder and the structure of the porous oxides is usually not related to the order of the organic template to start with, the "nanocasting" process introduced by Attard et al.[9] enables one to create a solidified inorganic copy of the original phase volume of the organic template, either as a homogeneous film or as a monolithic object. "Nanocasting" is a high-concentration synthesis, where lyotropic liquid crystalline phases, derived from surfactants or, later, block copolymers[10] and other colloidal templates, such as polymer dispersions[11] are used as structure-directing agents (templates).

Throughout these and the following investigations, it was demonstrated that copying from soft into hard matter can be extremely precise and can have a resolution below 1 nm. The only prerequisite for a successful performance of nanocasting is that the hydrolyzed silica precursor in the aqueous phase must not disturb the original order or the conformation of the organic templates, which is usually ensured by appropriate chemical choice of functional groups or adjustment of the interface energy between the two phases. It was shown for polystyrene-*b*-poly(ethylene oxide) (PEO) block copolymer aggregates that the small-angle scattering diffrac-

* To whom correspondence should be addressed. Fax: +49 331 567 9502. E-mail: han@mpikg-golm.mpg.de. Permanent address: Department of Chemistry, Nankai University, Tianjin 300071, China. E-mail: bhan@nankai.edu.cn.

(1) (a) Beck, J. S.; Vartuli, J. C. *Curr. Opin. Solid State Mater. Sci.* **1996**, *1*, 76−87. (b) Kresge, C. T.; Leonowicz, M. E.; Roth, W. J.; Vartuli, J. C.; Beck, J. S. *Nature* **1992**, *359*, 710−712. (c) Beck, J. S.; Vartuli, J. C.; Roth, W. J.; Leonowicz, M. E.; Kresge, C. T.; Schmitt, K. D.; Chu, C. T.-W.; Olson, D. H.; Sheppard, E. W.; McCullen, S. B.; Higgins, J. B.; Schlenker, J. L. *J. Am. Chem. Soc.* **1992**, *114*, 10834−10843. (d) Beck, J. S.; Vartuli, J. C.; Kennedy, G. J.; Kresge, C. T.; Roth, W. J.; Schramm, S. E. *Chem. Mater.* **1994**, *6*, 1816−1821. (e) Vartuli, J. C.; Schmitt, K. D.; Kresge, C. T.; Roth, W. J.; Leonowicz, M. E.; McCullen, S. B.; Hellring, S. D.; Beck, J. S.; Schlenker, J. L.; Olson, D. H.; Sheppard, E. W. *Chem. Mater.* **1994**, *6*, 2317−2326.

(2) Barton, T. J.; Bull, L. M.; Klemperer, W. G.; Loy, D. A.; McEnaney, B.; Misono, M.; Monson, P. A.; Pez, G.; Scherer, G. W.; Vartuli, J. C.; Yaghi, O. M. *Chem. Mater.* **1999**, *11*, 2633−2656.

(3) Hüsing, N.; Schubert, U. *Angew. Chem., Int. Ed.* **1998**, *37*, 21−45; *Angew. Chem.* **1998**, *110*, 22−47.

(4) (a) Ozin, G. A. *Adv. Mater.* **1992**, *4*, 612−649. (b) Ozin, G. A.; Chomski, E.; Khushalani, D.; MacLachlan, M. J. *Curr. Opin. Colloid Interface Sci.* **1998**, *3*, 181−193. (c) Ozin, G. A. *Can. J. Chem.* **1999**, *77*, 2001−2014. (d) Soten, I.; Ozin, G. A. *Curr. Opin. Colloid Interface Sci.* **1999**, *4*, 325−337. (e) Oliver, S.; Kuperman, A.; Ozin, G. A. *Angew. Chem., Int. Ed.* **1998**, *37*, 46−62; *Angew. Chem.* **1998**, *110*, 48−64.

(5) (a) Yang, P.; Zhao, D.; Margolese, D. I.; Chmelka, B. F.; Stucky, G. D. *Nature* **1998**, *396*, 152−155. (b) Zhao, D.; Yang, P.; Huo, Q.; Chmelka, B. F.; Stuchy, G. D. *Curr. Opin. Solid State Mater. Sci.* **1998**, *3*, 111−121.

(6) (a) Tanev, P. T.; Pinnavain, T. J. *Science* **1995**, *267*, 865−867. (b) Bagshaw, S. A.; Prouzet, E.; Pinnavaia, T. J. *Science* **1995**, *269*, 1242−1244. (c) Bagshaw, S. A.; Pinnavaia, T. J. *Angew. Chem., Int. Ed. Engl.* **1996**, *35*, 1102−1105. (d) Tanev, P. T.; Pinnavain, T. J. *Science* **1996**, *271*, 1267−1269. (e) Zhang, W.; Fröba, M.; Wang, J.; Tanev, P. T.; Wong, J.; Pinnavaia, T. J. *J. Am. Chem. Soc.* **1996**, *118*, 9164−9171. (f) Tanev, P. T.; Pinnavaia, T. J. *Chem. Mater.* **1996**, *8*, 2068−2079. (g) Zhang, W.; Pauly, T. R.; Pinnavaia, T. J. *Chem. Mater.* **1997**, *9*, 2491−2498. (h) Prouzet, E.; Pinnavaia, T. J. *Angew. Chem., Int. Ed. Engl.* **1997**, *36*, 516−518; *Angew. Chem.* **1997**, *109*, 533−536. (i) Tanev, P. T.; Butruille, J.-R.; Pinnavaia, T. J. In *Chemistry of Advanced Materials: An Overview*; Interrante, L. V., Hampden-Smith, M. J., Eds.; Wiley-VCH: New York, 1998; pp 329−388. (j) Pauly, T. R.; Liu, Y.; Pinnavaia, T. J.; Billinge, S. J. L.; Rieker, T. P. *J. Am. Chem. Soc.* **1999**, *121*, 8835−8842. (k) Mercier, L.; Pinnavaia, T. J. *Chem. Mater.* **2000**, *12*, 188−196.

(7) (a) Antonelli, D. M.; Ying, J. Y. *Curr. Opin. Colloid Interface Sci.* **1996**, *1*, 523−529. (b) Ying, J. Y.; Mehnert, C. P.; Wong, M. S. *Angew. Chem., Int. Ed.* **1999**, *38*, 56−77; *Angew. Chem.* **1999**, *111*, 58−82.

(8) Antonietti, M.; Göltner, C. G. *Angew. Chem., Int. Ed. Engl.* **1997**, *36*, 910−928; *Angew. Chem.* **1997**, *109*, 944−964.

(9) Attard, G. S.; Glyde, J. C.; Göltner, C. G. *Nature* **1995**, *378*, 366−368.

(10) Göltner, C. G.; Antonietti M. *Adv. Mater.* **1997**, *9*, 431−436.

(11) Antonietti, M.; Berton, B.; Göltner, C. G.; Hentze, H. P. *Adv. Mater.* **1998**, *10*, 154−159.

10.1021/cm0113088 CCC: $22.00
Published on Web 07/12/2002

togram (and therefore the spatial order) is kept throughout the solidification process; subsequent removal of the template by calcination results in a slight shrinkage due to the completion of silica condensation, but the structure is still preserved.[12] For a variety of cross-linkable polybutadiene-*b*-poly(ethylene oxide) block copolymers, it was even possible to compare directly the microtomed original, but a cross-linked phase with their silica replicas and a strict coincidence down to the finest structural details was found.[13]

Meanwhile, this technique has been used to depict fine structural details of the assemblies of block copolymer with one ionic polyelectrolyte block (both anionic and cationic),[14] to analyze delicate transition states between lamellar and hexagonal mesophases including observation of formerly unknown structural details.[15,16]

Therefore, nanocasting has been proved to be a valuable analytical technique to learn about the structure of complex interacting polymer systems or colloids in water. Its main advantage is the possibility analyzing a delicate and fragile, not cuttable and badly contrasted complex fluid by its solidified, and therefore permanent, well-contrasted and cuttable "hardcopy".

Cyclodextrins are cyclic oligosaccharides consisting of six, seven, or eight α(1→4)-linked glucopyranose units (α-, *β*-, or *γ*-cyclodextrin, respectively). The primary hydroxyl groups on C-6 of the glucose residues lie on the narrow side of the formed torus, while the secondary hydroxyl groups on C-2 and C-3 are located on the wide side. This makes the inner surface of the toroidal cavity hydrophobic, while the exterior surface is hydrophilic.[17,18] A vast variety of hydrophobic molecules which have only limited solubility in aqueous media like alkanes or aromatic systems can "dissolve" in water via the formation of inclusion complexes with the cyclodextrins due to the strong binding affinity.[19−22] The stability of the complexes depends on many factors such as the size/shape fit, hydrophobic interaction, hydrogen bonding, electrostatic interactions, and/or the surrounding solution. For further details of the complexation mechanism, see the literature.[23]

In a related recent work, we have shown that, using the nanocasting concept, cyclodextrins can act as templates for the production of porous silica materials with pore size exactly resembling the cyclodextrin diameters (1.5−2 nm) and a bicontinuous "worm-type" pore structure.[24] The pores are very uniform, and no further microporosity was found as results when silica is prepared by templating of block copolymers.[25] Another set of experiments had described the employment of inclusion complexes between cyclodextrins and organometallics as templates for silica nanocasting as a convenient way to synthesize fine and well-defined metal nanoparticles in a porous silica support by a one-step synthesis.[26]

Suitable linear polymer chains can penetrate through the cyclodextrin cavities to give pseudopolyrotaxane; if both of the ends are stopped by bulky groups, polyrotaxanes are obtained.[27] Wenz and co-workers[28] reported the preparation of several pseudopolyrotaxanes based on α-cyclodextrin and polyamines. Harada[29] reported the syntheses of several crystalline (pseudo)polyrotaxanes (inclusion complexes), the so-called "molecular necklace", and the polyrotaxanes stopped by bulky groups in both ends. Harada et al.[30] and Tonelli et al.[31] obtained pseudopolyrotaxanes of cyclodextrins with poly(*ϵ*-caprolactone) and nylon 6. In the present contribution, we want to address the question of whether these kinds of supramolecular structures of cyclodextrins, where the assembly is driven by inclusion complexation, can also be depicted by the nanocasting process. The material science aspect in this research is that, vice versa, pore structure and connectivity is established and controlled by the supramolecular complexation process in itself, which would allow a rational pore design based on the concepts of supramolecular chemistry. For the beginning, we want to focus on poly(ethylene glycol), which is known to form linear crystalline inclusion complexes with α-cyclodextrins,[29d,32] and poly(propylene glycol), which relies on *β*-cyclodextrins to complex with.[33] The structural models proposed by Harada[29] for the resulting pseudopolyrotaxanes are depicted in Figure 1. In addition, we will also examine the complexes between nonionic surfactants and cyclodextrins, where both the hydrophilic and the hydrophobic parts of the

(12) Göltner, C. G.; Henke, S.; Weissenberger, M. C.; Antonietti, M. *Angew. Chem., Int. Ed.* **1998**, *37*, 613−616; *Angew. Chem.* **1998**, *110* (5), 633−636.
(13) Hentze, H. P.; Krämer, E.; Berton, B.; Förster, S.; Antonietti, M.; Dreja, M. *Macromolecules* **1999**, *32*, 5803−5809.
(14) Krämer, E.; Förster, S.; Göltner, C.; Antonietti, M. *Langmuir* **1998**, *14*, 2027−2031.
(15) Göltner, C. G.; Berton, B.; Krämer, E.; Antonietti, M. *Chem. Commun.* **1998**, 2287−2288.
(16) Göltner, C. G.; Berton, B.; Kämer, E.; Antonietti, M. *Adv. Mater.* **1999**, *11*, 395−398.
(17) Szejtli, J., Osa, T., Eds. *Comprehensive Supramolecular Chemistry: Cyclodextrins*; Pergamon: Oxford, U.K., 1996; Vol. 3.
(18) (a) Szejtli, J. *Cyclodextrin and their Inclusion Complexation*; Aka-demia Kiado: Budapest, 1982. (b) Bender, M. L.; Komiyama, M. *Cyclodextrin Chemistry*; Springer-Verlag: Berlin, 1978.
(19) Saenger, W. *Angew. Chem., Int. Ed. Engl.* **1980**, *19*, 344−362; *Angew. Chem.* **1980**, *92*, 343−361.
(20) Connors, K. A. *Chem. Rev.* **1997**, *97*, 1325−1357.
(21) Schneider, H.-J.; Hacket, F.; Rüdiger, V.; Ikeda, H. *Chem. Rev.* **1998**, *98*, 1755−1785.
(22) Liu, Y.; Han, B.-H.; Sun, S.-X.; Wada, T.; Inoue, Y. *J. Org. Chem.* **1999**, *64*, 1487−1493.
(23) (a) Inoue, Y.; Wada, T. In *Advances in Supramolecular Chemistry*; Gokel, G. W., Ed.; JAI Press: Greenwich, CT, 1997; Vol. 4, pp 55−96. (b) Rekharsky, M. V.; Inoue, Y. *Chem. Rev.* **1998**, *98*, 1875−1917. (c) Liu, Y.; Han, B.-H.; Li, B.; Zhang, Y.-M.; Zhao, P.; Chen, Y.-T.; Wada, T.; Inoue, Y. *J. Org. Chem.* **1998**, *63*, 1444−1454.
(24) Polarz, S.; Smarsly, B.; Bronstein, L.; Antonietti, M. *Angew. Chem., Int. Ed.* **2001**, *40*, 4417−4421; *Angew. Chem.* **2001**, *113*, 4549−4553.
(25) (a) Göltner, C.; Smarsly, B.; Berton, B.; Antonietti, M. *Chem. Mater.* **2001**, *13*, 1617−1624. (b) Smarsly, B.; Göltner, C.; Antonietti, M.; Ruland, W.; Hoinkis, E. *J. Phys. Chem. B* **2001**, *105*, 831−840.
(26) Han, B.-H.; Polarz, S.; Antonietti, M. *Chem. Mater.* **2001**, *13*, 3915−3919.
(27) Wenz, G. *Angew. Chem., Int. Ed. Engl.* **199**4, *3*3, 803−822; *Angew. Chem.* **1994**, *106*, 851−870.
(28) (a) Wenz, G.; Keller, B. *Angew. Chem., Int. Ed. Engl.* **1992**, *31*, 197−199; *Angew. Chem.* **1992**, *104*, 201−204. (b) Wenz, G.; Keller, B. In *Minutes of the 6th International Symposium on Cyclodextrins*; Hedges, A. R., Ed.; Editions de Santé: Paris, 1992; pp 192−197. (c) Wenz, G.; von derBey, E.; Schmidt, L. *Angew. Chem., Int. Ed. Engl.* **1992**, *31*, 783−785; *Angew. Chem.* **1992**, *104*, 758−761. (d) Wenz, G.; Keller, B. *Polym. Prepr. (Am. Chem. Soc., Div. Polym. Chem.)* **1993**, *34*, 62−63. (e) Meier, L. P.; Heule, M.; Caseri, W. R.; Shelden, R. A.; Suter, U. W.; Wenz, G.; Keller, B. *Macromolecules* **1996**, *29*, 718−723. (f) Weickenmeier, M.; Wenz, G. *Macromol. Rapid Commun.* **1997**, *18*, 1109−1115. (g) Herrmann, W.; Keller, B.; Wenz, G. *Macromolecules* **1997**, *30*, 4966−4972.
(29) (a) Harada, A. *Polym. News* **1993**, *18*, 358−363. (b) Harada, A. In *Large Ring Molecules*; Semlyen, J. A., Ed.; Wiley: Chichester, U.K., 1996; pp 407−432. (c) Harada, A. *Adv. Polym. Sci.* **1997**, *133*, 141−191. (d) Harada, A. *Coord. Chem. Rev.* **1996**, *148*, 115−133.
(30) Kawaguchi, Y.; Nishiyama, T.; Okada, M.; Kamachi, M.; Harada, A. *Macromolecules* **2000**, *33*, 4472−4477.
(31) Rusa, C. C.; Luca, C.; Tonelli, A. E. *Macromolecules* **2001**, *34*, 1318−1322.

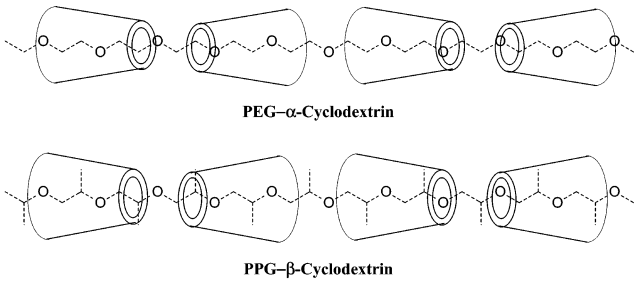

Figure 1. Pseudopolyrotaxanes based on α-MCD with PEO and *β*-MCD with PPO.

surfactant can enter and bind to the cyclodextrin cavity. In addition, a block copolymer of the type PEO-*b*-PPO-*b*-PEO (Pluronics; PPO = poly(propylene oxide) is analyzed, where complexation with cyclodextrins is expected to change the self-assembly behavior.

Experimental Section

Methyl-α-cyclodextrin (α-MCD) and methyl-*β*-cyclodextrin (*β*-MCD) were provided by the Wacker-Chemie AG/Germany. The degree of substitution is 1.6−1.9 and 1.7−1.9 per anhydro glucose unit for α-MCD and *β*-MCD, respectively. Therefore, the calculated average molecular weight is ca. 1120 g mol^{-1} (α-MCD) and 1310 g mol^{-1} (*β*-MCD). Their solubilities in water are much larger than the corresponding native cyclodextrins (α-MCD, >300 g in 100 mL of water; *β*-MCD, >200 g in 100 mL of water).

The following chemicals were obtained from Fluka: Brij 30 [main component: tetraethylene glycol dodecyl ether, $CH_3(CH_2)_{11}(OCH_2CH_2)_4OH$], Brij 35P [main component: tricosaethylene glycol dodecyl ether, $CH_3(CH_2)_{11}(OCH_2CH_2)_{23}OH$], Brij 56 [main component: decaethylene glycol hexadecyl ether, $CH_3(CH_2)_{15}(OCH_2CH_2)_{10}OH$], Brij 78 [main component: eicosaethylene glycol octadecyl ether, $CH_3(CH_2)_{17}(OCH_2CH_2)_{20}OH$], and PEG 600 [poly(ethylene glycol), average M_n ca. 600, EO number ca. 13.2].

The following chemicals were purchased from Aldrich: PEG 2000 [poly(ethylene glycol), average M_n ca. 2000, EO number ca. 45.0], PEG 10000 [poly(ethylene glycol), average M_n ca. 10 000, EO number ca. 226.9], PPG 725 [poly(propylene glycol), average M_n ca. 725, PO number ca. 12.2], PPG 1000 [poly(propylene glycol), average M_n ca. 1000, PO number ca. 16.9], PPG 2000 [poly(propylene glycol), average M_n ca. 2000, PO number ca. 34.2], PPG 2700 [poly(propylene glycol), average M_n ca. 2700, PO number ca. 46.2], PPG 4000 [poly(propylene glycol), average M_n ca. 4000, PO number ca. 68.7], and poly(ethylene glycol)-*block*-poly(propylene glycol)-*block*-poly(ethylene glycol) [EOPOEO; Pluronics F-68, average M_n ca. 8400, $EO_{76}PO_{29}EO_{76}$].

A hydrochloride acid solution (0.10 M, Merck) and pure water (5.5 μS/m) are used to prepare the solution (pH 2.0, 3.0, and 4.0). Tetramethyl orthosilicate (TMOS; 99+%) was purchased from Fluka and Aldrich. Triton X-405 (70% solution of tetracontaethylene glycol *tert*-octylphenyl ether in water) was obtained from Ferak Berlin.

All of the chemicals mentioned above were used without further purification.

Instead of using only the pure cyclodextrins and cyclodextrin complexes with organometallics as in refs 24 and 26, the methylated cyclodextrins are modified by building supramolecular assemblies (pseudopolyrotaxane) with oligo/poly(ethylene oxide) (EO) containing nonionic surfactants, poly(ethylene glycol) (PEG), poly(propylene glycol) (PPG), and poly(ethylene oxide) and poly(propylene oxide) (PO) containing triblock copolymer (Pluronics F-68). A total of 2.0 mmol α-MCD or *β*-MCD was dissolved in an aqueous pH 2.0, 3.0, or 4.0 hydrochloride acid solution (the concentration of MCD is ca. 40 wt %) under stirring. To the clear solution was added an equivalent (molar) amount of polymer, i.e., one cyclodextrin ring unit to two EO or PO groups,[30] which was stirred overnight in order to obtain a clear solution.

After filtration (syringe filter of 5 μm), this solution is directly taken without further treatment for the nanocasting.[16] The double amount (weight) of TMOS with respect to MCD is added under stirring. The mixture is continuously stirred until the homogenization is reached (ca. 1, 10, and 60 min at pH 2.0, 3.0, and 4.0, respectively). The methanol formed during hydrolysis is removed via evaporation under reduced pressure until thick transparent gels are obtained. The gels are aged in open flasks at room temperature for about 1 week.

The resulting silica materials were calcined in an oven at 500 °C (2 h for a temperature rise) with flows of nitrogen (6 h) and oxygen (8 h).

The following methods were applied for analysis: transmission electron microscopy (TEM) images were acquired on a Zeiss EM 912 Omega TEM at an acceleration voltage of 120 kV. Samples were ground in an agate ball mill and taken up in absolute ethanol. One droplet of the suspension was applied to a 400 mesh carbon-coated copper grid and left to dry in air. Nitrogen sorption ($T = -196$ °C) data were obtained with a Micromeritics Tristar 3000 automated gas adsorption analyzer. Before sorption measurement, the samples were degassed in a Micromeritics VacPrep061 degasser overnight at 150 °C under 100 μTorr pressure. Isotherms were evaluated with the Barrett−Joyner−Halenda (BJH) theory to give the pore parameters, including surface areas, pore size, and its distribution.

Small-angle X-ray scattering (SAXS) curves were recorded on a rotating-anode instrument with pinhole collimation. A Nonius rotating anode ($P = 4$ kW, Cu Kα) and an image-plate detector system were used with respect to the pinhole system. With the image plates placed at a distance of 40 cm from the sample, a scattering vector range from $s = 0.05$ to 1.6 nm^{-1} was available [$s = (2 \sin \theta)/\lambda$, 2θ scattering angle, $\lambda = 0.154$ 18 nm]. The samples were irradiated for 24 h to reduce the noise level and to obtain a sufficiently high scattering intensity. Two-dimensional diffraction patterns were transformed into a one-dimensional radial average of the scattering intensity.

Results and Discussion

1. PEO−α-MCD-Based Silicas. For a first characterization, the as-prepared materials have been investigated with TEM. In all cases, the TEM images verify the optical impression that the material is homogeneous (i.e., no demixing occurred throughout the process), and wormlike pore structures were observed. After calcinations, the porous architecture remained in all investigated silica materials.

Interestingly, the pore size of the resulting porous silica depends on the pH values of the sol−gel recipe, more or less depending on the included material. This is shown in Figure 2 where the three samples made with α-MCD and PEG 2000 condensed at pH 2.0, 3.0, and 4.0 under otherwise unaltered conditions are compared with each other. Usually, the structure of the formed silica does not change that strongly in the range of pH

(32) (a) Harada, A.; Kamachi, M. *Macromolecules* **1990**, *23*, 2821−2823. (b) Harada, A.; Li, J.; Kamachi, M. *Nature* **1992**, *356*, 325−327. (c) Harada, A.; Li, J.; Kamachi, M. *Nature* **1993**, *364*, 516−518. (d) Harada, A.; Li, J.; Kamachi, M. *Macromolecules* **1993**, *26*, 5698−5703. (e) Harada, A.; Li, J.; Kamachi, M. *J. Am. Chem. Soc.* **1994**, *116*, 3192−3196. (f) Li, J.; Harada, A.; Kamachi, M. *Polym. J.* **1994**, *26*, 1019−1026. (g) Li, J.; Harada, A.; Kamachi, M. *Bull. Chem. Soc. Jpn.* **1994**, *67*, 2808−2818. (h) Harada, A.; Li, J.; Kamachi, M. *Macromolecules* **1994**, *27*, 4538−4543.

(33) Harada, A.; Kamachi, M. *J. Chem. Soc., Chem. Commun.* **1990**, 1322−1323.

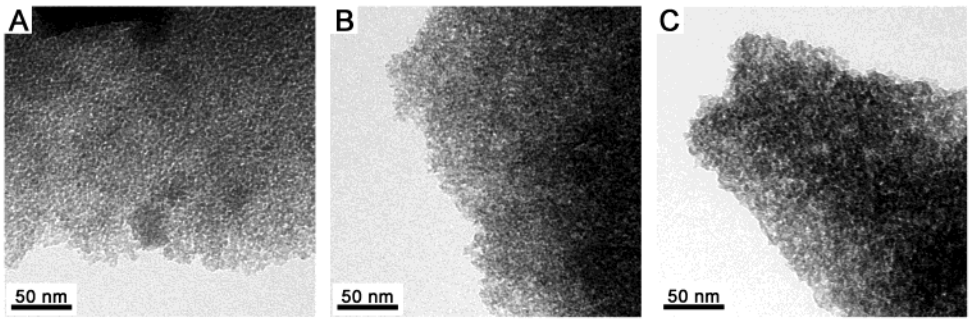

Figure 2. TEM images of three silicas made from α-MCD and PEG 2000 condensed at pH 2.0 (A), 3.0 (B), and 4.0 (C). The light area corresponds to the pores, while the dark area corresponds to walls.

2.0−4.0,[34,35] so it is deduced that we observe a pH-dependent property of the template.

From the TEM images, e.g., shown in Figure 2, it is seen that the pore structure differs from those of pure cyclodextrin-based silicas.[24] For the present pore structures resulting from cyclodextrin pseudopolyrotaxanes, generally, short tubelike pores are observed. (Figure 2) The short tubelike pore structures of the silica materials at pH 2.0 definitely stem from the nanocasting of the cylindrical shape of the cyclodextrin pseudopolyrotaxanes. This structure ("molecular necklace" or string of beads;[29a,32b] see Figure 1) has already been observed by scanning tunneling microscopy (STM) for the system of α-cyclodextrin and PEG.[36] The coarsening of the pore structures with increasing pH values is interesting and indicates that the template increases in size. This observation, however, is consistent with a structure model proposed by Harada et al. for the cyclodextrin−PEG gel in neutral media,[32f] where pseudopolyrotaxane domains aggregate toward bundles. Evidently, the pH values influence the aggregation process, and this can be followed by the development of the pore size.

As a control experiment, the silica materials made by the pure α-MCD show only the typical small influence from pH 2.0 to 4.0.

Nitrogen sorption experiments performed at the same set of materials indeed show an increase in the pore diameter with increasing pH values, as shown in Figure 3 for the silica materials based on α-MCD and PEG 2000, in which the pore size distributions from the desorption branches of the isotherms are inlet.

Generally, the material made at pH 2.0 shows the typical isotherm of a porous silica with pores at the borderline between micro- and mesoporosity,[37] as is the case for the bare cyclodextrin-based silicas, and the average pore diameter is about 2 nm. The pore confirmed the imprint of single pseudopolyrotaxane domains. With increasing pH values, the pseudopolyrotaxane domains tend to form aggregates, and larger average pore sizes are created by the nanocasting process. Therefore, an additional mesoporosity develops which becomes the dominant structure element at pH 4.0 (diameter of ca. 3.8 nm for the system based on α-MCD and PEG 2000; see Figure 3). From the inlets in Figure 3, it is easy to see that the pore size increases and the pore size distributions from the desorption branches of the isotherms become narrower with in-

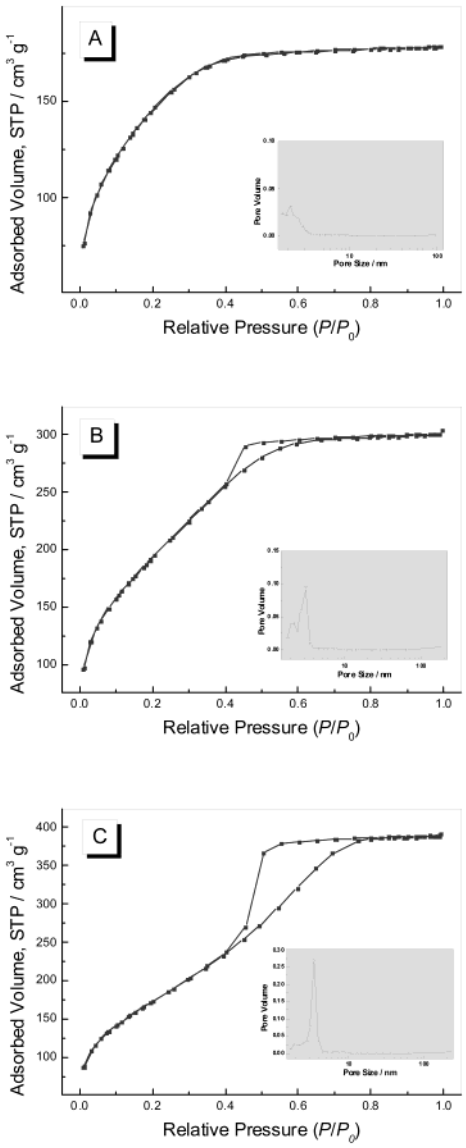

Figure 3. Nitrogen sorption data of three silicas made from α-MCD and PEG 2000 condensed at pH 2.0 (A), 3.0 (B), and 4.0 (C). Inlets: pore size distribution, as calculated by the BJH theory from the desorption branch.

(34) Iler, R. K. *The Chemistry of Silica: Solubility, Polymerization, Colloid and Surface Properties, and Biochemistry*; John Wiley & Sons: New York, 1979.

(35) Brinker, C. J.; Scherer, G. W. *Sol−Gel Science: The Physics and Chemistry of Sol−Gel Processing*; Academic Press: San Diego, 1990.

(36) Shigekawa, H.; Miyake, K.; Sumaoka, J.; Harada, A.; Komiyama, M. *J. Am. Chem. Soc.* **2000**, *122*, 5411−5412.

(37) (a) Gregg, S. J.; Sing, K. S. W. *Adsorption, Surface Area and Porosity*, 2nd ed.; Academic Press: London, 1982. (b) Sing, K. S. W.; Everett, D. H.; Haul, R. A. W.; Moscou, L.; Pierotti, R. A.; Rouquérol, J.; Siemieniewska, T. *Pure Appl. Chem.* **1985**, *57*, 603−619.

Table 1. Nitrogen Sorption Data for Porous Silicas Obtained from α-MCD and PEO Containing Nonionic Surfactants and Glycols at pH 2.0, 3.0, and 4.0, Respectively

	pH 2.0			pH 3.0			pH 4.0		
	pore diameter (nm)	BET surface area (m^2/g)	pore volume (cm^3/g)	pore diameter (nm)	BET surface area (m^2/g)	pore volume (cm^3/g)	pore diameter (nm)	BET surface area (m^2/g)	pore volume (cm^3/g)
pure α-MCD	1.88	608	0.286	2.02	699	0.354	2.49	698	0.435
PEG 600	2.04	539	0.274	2.82	559	0.394	3.27	596	0.487
PEG 2000	1.98	588	0.290	2.60	715	0.464	3.77	639	0.601
PEG 10000	1.98	540	0.267	2.53	561	0.355	3.48	596	0.520
Brij 30	1.95	595	0.289	2.83	598	0.422	4.27	608	0.648
Brij 35P	1.97	540	0.266	2.03	760	0.386	3.50	640	0.560
Brij 56	1.96	585	0.286	2.26	616	0.348	3.41	623	0.532
Brij 78	1.91	615	0.294	2.30	647	0.372	3.72	636	0.591
Triton X-405	2.14	557	0.299	2.13	744	0.397	3.29	967	0.797

creasing pH values, while the adsorption pore size distributions are hardly comparable (not shown). The pronounced hysteresis is the typical feature of mesoporous materials, in which the pores are interconnected by a smaller opening ("inkbottle" effect).[34]

The porosity data obtained at all α-MCD inclusion compound species are summarized in Table 1. When the isotherms and the resulting pore parameters with the bare cyclodextrin samples at pH 2.0 are compared, it is seen that the materials have about the same Brunauer−Emmett−Teller (BET) surface area, average pore size, and pore volume. This means that the PEO chains do not seem to create any additional microporosity, as they would do by themselves in a silica recipe.[25] However, as pointed out by Harada and Kamachi,[32f] in the α-MCD and PEG aqueous solution, besides the dominant pseudopolyrotaxanes, we have to expect that there are minor amounts of partially unincluded PEG chains and unthreaded cyclodextrin units because of the thermodynamic threading−dethreading equilibrium. Although this possibly creates some additional microporosity, on the other hand, the formation of the pseudopolyrotaxanes possessing higher order than the pure cyclodextrin system would contribute to a decrease in the microporosity. Therefore, no hint for the typical molecular microporosity of PEO is found in the data, which further explicitly proves that at least most PEO chains indeed form pseudopolyrotaxanes by inclusion complexation with α-MCD and that the nanocasting process replicates this supramolecular morphology of a cylindrical string of beads.

A more careful comparison of the porosity data in Table 1 shows that the average pore size increases upon increasing pH values (Figure 3, inlets) but that the pore volume increases, too, and the BET surface area also shows an "increase" tendency. This is somewhat counterintuitive (note that the relative composition of template to wall material is constant all over the sample set). We think there are three possible contributions. First, we attribute this effect partially to a successively lower shrinking of the high pH materials, which is composed not only of larger and thicker walls (vide post, SAXS evaluation) but also of a change in the connectivity between the silica networks. This makes both the capillary pressures and the compressibility of the walls lower, i.e., the porous silica more resistant against collapse. It is underlined that the porosity of the pH 4.0 materials is just slightly below the ideal one calculated from stoichiometry, whereas all other materials are significantly lower.

Second, with regards to the template, the origins for this pH effect on the pore structure seem to be hard to identify because the binding constants of cyclodextrin inclusion complexes usually do not depend that strongly on the pH value.[23b,38] However, just as was already discussed (vide supra), the pH value is sure to influence the aggregation of the pseudopolyrotaxane domains, and the Harada model is based on the system in neutral media (pH 7.0).[32f] Although there is no report on the pH effect on the hydrogen bonding,[39] we think that a higher pH value would enhance the hydrogen bonding involving cyclodextrin units in a given pH range (pH 2.0−4.0), which is embodied in the hydrogen bonding of inter-rotaxane and/or between the pseudopolyrotaxanes and the surrounding water molecules (Figure 4). This contributes to the seemingly counterintuitive increases in the average pore size, surface area, and pore volume. In fact, we also could find these tendencies in pure cyclodextrin systems; however, they are less pronounced than those in the pseudopolyrotaxane systems. However, in some cases, the BET surface areas at pH 4.0 are less than those at pH 3.0, where this tendency may be canceled by the pore size increase effect (when the pore size increases, the BET surface area should decrease on the basis of the same amount of a template).

Finally, because the isoelectronic point for silica is at pH 2.0, silica condensation is the slowest at pH 2.0. At higher pH values, condensation is remarkably hastened, which causes more compact condensation structures,[34,35] also contributing to a higher mechanical resistance of the pore walls against shrinkage.

On the basis of these experiments (Table 1), both the length of the PEO chain and a possible hydrophobic anchor were varied over a broad range. Somewhat surprisingly, the structural variations do not evidently take effect on the pore structures, as compared with the pH effect. Especially, the pore structure is not sensitive to the changes of the length of PEO chains, i.e., the length of the pseudopolyrotaxanes. This is reasonable because the length of the PEO chains would not explicitly influence the formation of the pseudopolyrotaxanes and the aggregation of the pseudopolyrotaxane domains and thus would not seriously influence the porosity data. However, the fact that nonionic surfac-

(38) Liu, Y.; Han, B.-H.; Qi, A.-D.; Chen, R.-T. *Bioorg. Chem.* **1997**, *25*, 155−162.

(39) (a) Jeffrey, G. A.; Saenger, W. *Hydrogen Bonding in Biological Structures*; Springer-Verlag: Berlin, 1994. (b) Saenger, W. Private communication.

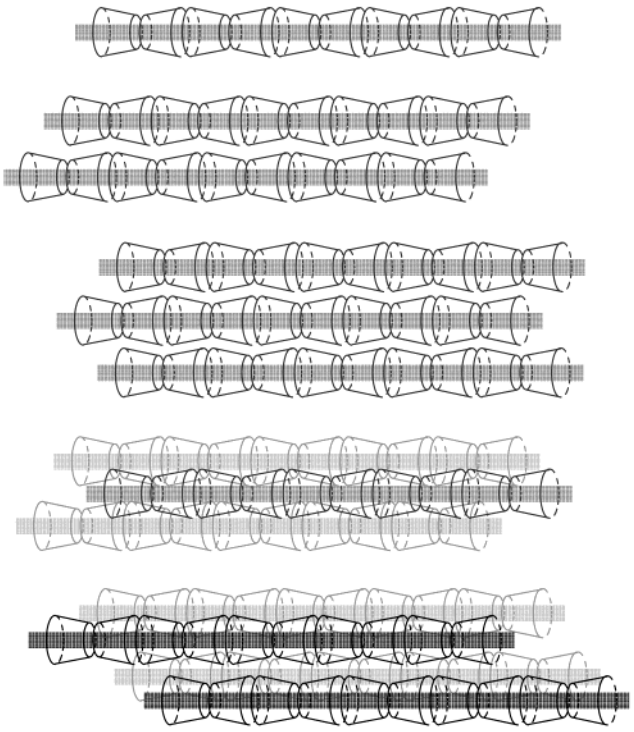

Figure 4. Schematics of the pH-dependent aggregation of pseudopolyrotaxanes of polyether with cyclodextrins. At pH 2.0, a single pseudopolyrotaxane domain predominates; with increasing pH values (pH 3.0 and 4.0), the aggregation of pseudopolyrotaxanes is enhanced to give bundle domains, and a small amount of unthreaded cyclodextrins is omitted.

tants do not create pores of the size of their micelles[6d,f,40] shows that they are well-included and cannot aggregate.

2. PPG−*β*-MCD-Based Silicas. The situation is simpler for the hydrophobic PPG, which is not water soluble and also does not mix with the silica phase. In this case, however, the pseudopolyrotaxanes have to be formed with the *β*-cylodextrins because accommodation of the pendant methyl group in the propylene oxide unit relies on a larger cavity.[29,33]

It is worth mentioning that PPG does not dissolve in an otherwise identically treated aqueous solution; its successful "dissolution" is therefore already a direct proof for the success of a nearly complete complexation. Interestingly, when the clear solution (*β*-MCD + PPG 2700) is diluted, phase separation occurs. This is due to the threading−dethreading complexation equilibrium shift, which gives more uncomplexed species (Le Chatelier Principle). Therefore, this further confirms the presence of the pseudopolyrotaxane at higher concentrations. Although we could not state that PPG chains are completely included in the *β*-cyclodextrin cavities under reaction conditions, the amount of unincluded polymer chains is certainly negligible.

All final silica samples are optically clear and also homogeneous in TEM observation, as shown in Figure 5 for the silica materials from *β*-MCD and PPG 2700, which means the PPG chains is not expelled or dethreaded throughout the experiment. TEM images support the aggregation picture found for the α-MCD systems at various pH values; i.e., the pore structure differs from the corresponding pure cyclodextrin systems, and the pore size increases with the increasing pH values. Nitrogen sorption isotherms are shown in Figure 6 for the same set silica materials. The resulting sorption data of the synthesized materials are summarized in Table 2.

The data in Table 2 and Figure 6 also nicely support the interpretation of the first set of data. For the *β*-MCD and PPG system, at low pH value, the nanocasting of the pseudopolyrotaxanes creates with remarkable stability short tubelike porous silicas with pore diameters of the size of the *β*-MCD molecule. Neither pore diameter and pore volume nor surface area depends on the molecular weight of the PPG chains. The fact that we do not observe any influence of the different lengths of the pseudopolyrotaxanes (PPG 725 has a contour length of about 5 nm and PPG 4000 a contour length of 27.5 nm) speaks that shorter pseudopolyrotaxanes might self-assemble to longer tubelike aggregates. At higher pH values, the aggregation of the pseudopolyrotaxanes leads to a larger average pore size too.

The higher order of the pseudorotaxane silicas as well as the bundle formation is also nicely seen in the SAXS data. Figure 7a shows the bare scattering data of *β*-MCD−PPG 2700 silica materials from the three different pH values, whereas Figure 7b depicts the transformation of the scattering curves into the so-called "chord length distribution" (CLD), as was discussed in refs 24 and 40.

The first peak of the CLD is in all cases at the same position and indicative of the cross section of a CLD unit. The fact that there is no pronounced contribution at shorter length scales and, in particular, the low value of $g(0)$ shows that indeed solvent pores or pores due to "naked" PPG polymer chains are negligible, i.e., indeed we template in all cases at the smallest primary cyclodextrin or pseudopolyrotaxane units.

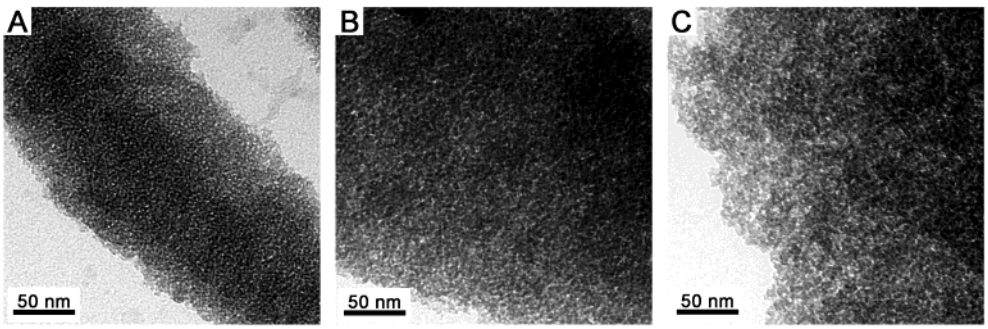

Figure 5. TEM images of three silicas made from *β*-MCD and PPG 2700 condensed at pH 2.0 (A), 3.0 (B), and 4.0 (C). The light area corresponds to the pores, while the dark area corresponds to walls.

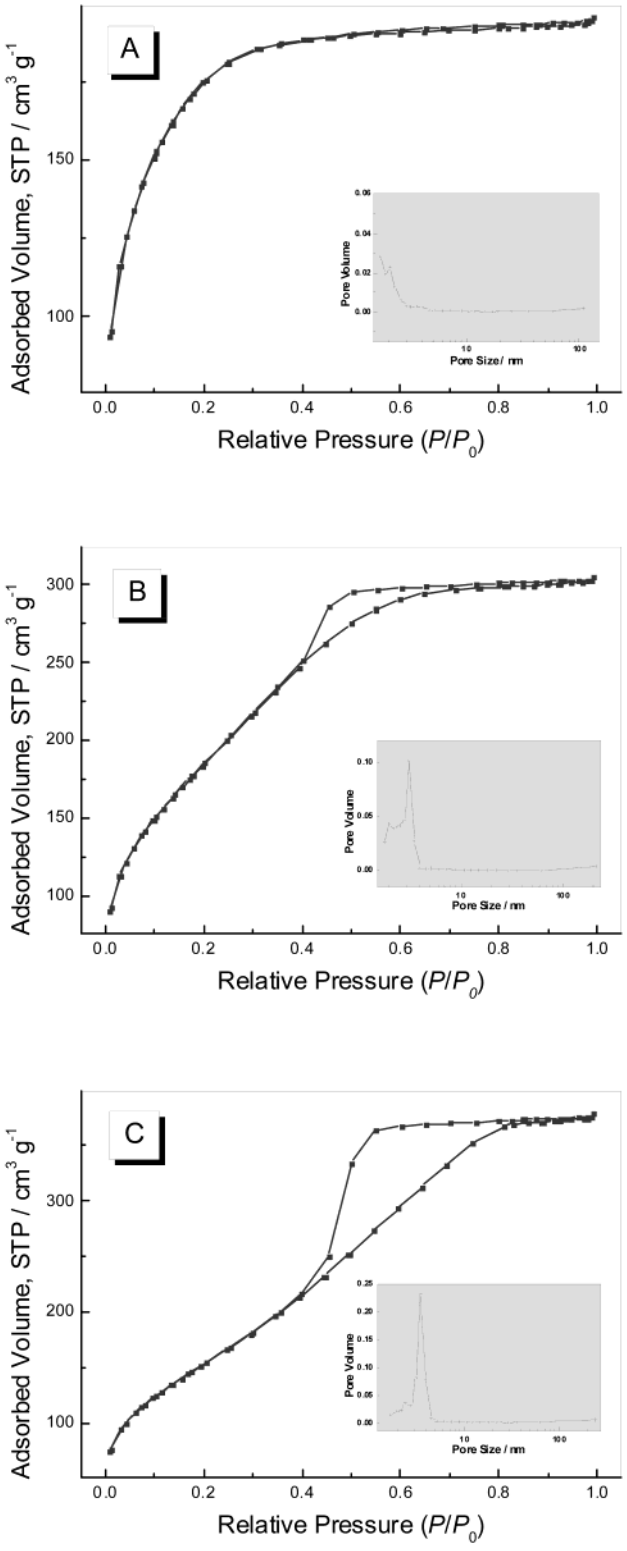

Figure 6. Nitrogen sorption data of three silicas made from β-MCD and PPG 2700 condensed at pH 2.0 (A), 3.0 (B), and 4.0 (C). Inlets: pore size distribution, as calculated by the BJH theory from the desorption branch.

For all pseudopolyrotaxane samples, we observe a second peak in the CLD at about 2 times the cyclodextrin diameter, which is only present as a shoulder in the silica sample casted from the bare cyclodextrin.[24] These well-pronounced CLD patterns by themselves indicate an increase of order in the pore system as was also observed by TEM and are, by some mathematical arguments, not due to an increased stiffness (which would lead to a tail in the CLD) but due to the parallel alignment of the pseudopolyrotaxane units. On the basis of the CLD evaluation, it could be concluded that at pH 2.0 a majority of the pseudopolyrotaxanes align in parallel and form dimers or smaller two-dimensional arrays (note that for a slit pore only the minimal extension is determined in gas adsorption experiments).

For the pH 3.0 and 4.0 samples, larger structures become increasingly important, as predicted by the Harada model (see Figure 4). In contrast to that at pH 2.0, the CLD curves show a tail toward larger sizes of up to 6 and 9 nm for pH 3.0 and 4.0, respectively, proving that the bundles become three-dimensional and can contain a larger number of pseudopolyrotaxane units.

The evaluation of the CLDs provides the average Porod length l_p, which is directly related to the average chord length ("pore size") l_{pore} of the pores and the average chord length l_{solid} of the solid ("wall thickness") by the relations

$$\frac{1}{l_p} = \frac{1}{(1-\phi)l_{pore}} = \frac{1}{\phi l_{solid}}$$

where ϕ is the porosity obtained from nitrogen sorption.[40] On the basis of this relationship, we calculated an increase in the average wall thickness l_{solid} from 2.7 nm (pH 2.0) to 4.2 nm (pH 3.0) and to 4.9 nm (pH 4.0) and in the average pore size l_{pore} from 1.8 nm (pH 2.0) to 3.1 nm (pH 3.0) and to 4.7 nm (pH 4.0), which is reasonably consistent with the data from the sorption measurement.

3. Block Copolymer−Cyclodextrin-Based Silicas. In a last set of experiments, inclusion complexes of block copolymer of the type PEO-*b*-PPO-*b*-PEO were formed. The somewhat curious fact behind these experiments is that each of the blocks just can bind one of the cyclodextrins; that is, PEO preferentially binds α-MCD, whereas PPO complexes exclusively with β-MCD.[29] This was also confirmed by a computational study: when α- and β-cyclodextrins are complexed on copolymer $(PO)_4$-$(EO)_4$, β-cyclodextrin is situated preferentially on the PO part of the polymer, whereas α-cyclodextrin is located on the EO branch of the polymer. The highly selective threading is mainly attributed to the relative stability.[41] β-Cyclodextrin fits tightly on the PO sites, whereas the highly constrained α-cyclodextrin rim is deformed when placed on PO parts.[29d,31,36] Addition of bare α-MCD therefore would leave the hydrophobic PO block of the copolymers uncomplexed and just change the aggregation behavior of the resulting supramolecular assemblies. Addition of bare β-MCD, on the other hand, would result in a purely hydrophilic structure, where however the PEO should be uncomplexed and should create molecular pores. Yui and co-workers[42] reported the synthesis of pseudopolyrotaxanes and polyrotaxanes from β-cyclodextrin and PEO−PPO−PEO triblock copolymer (Pluronics P-84). The obtained pseudopolyrotaxane contains ca. 17 β-cyclodextrin units,

(40) Smarsly, B.; Polarz, S.; Antonietti, M. *J. Phys. Chem. B* **2001**, *105*, 10473−10483.
(41) Mayer, B.; Klein, Ch. Th.; Topchieva, I. N.; Köhler, G. *J. Comput.-Aided Mol. Des.* **1999**, *136*, 373−383.

Table 2. Nitrogen Sorption Data for Porous Silicas Obtained from β-MCD and PPG at pH 2.0, 3.0, and 4.0, Respectively

	pH 2.0			pH 3.0			pH 4.0		
	pore diameter (nm)	BET surface area (m^2/g)	pore volume (cm^3/g)	pore diameter (nm)	BET surface area (m^2/g)	pore volume (cm^3/g)	pore diameter (nm)	BET surface area (m^2/g)	pore volume (cm^3/g)
pure β-MCD	1.89	659	0.311	2.14	778	0.410	2.58	804	0.4936
PPG 725	1.88	584	0.274	3.40	579	0.491	4.50	538	0.606
PPG 1000	1.88	607	0.285	3.50	596	0.519	3.41	582	0.496
PPG 2000	1.88	565	0.265	3.17	662	0.521	3.29	614	0.506
PPG 2700	1.89	617	0.292	2.72	687	0.467	4.08	569	0.579
PPG 4000	2.02	604	0.305	2.64	687	0.453	6.19	449	0.694

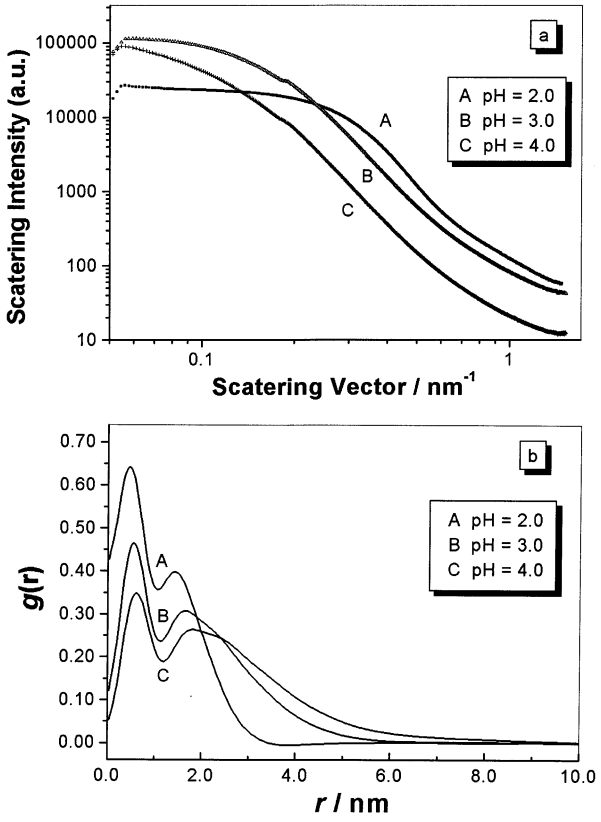

Figure 7. (a) SAXS diffractograms of three silica materials prepared from β-MCD and PPG 2700 condensed at pH 2.0 (A), 3.0 (B), and 4.0 (C). (b) CLD for the three silica materials prepared from β-MCD and PPG 2700 condensed at pH 2.0 (A), 3.0 (B), and 4.0 (C) ($g(r)$ = CLD function; r = radius).

which is close to the stoichiometric number, i.e., ca. 19.4 assuming that one β-cyclodextrin molecular is threaded onto two repeating propylene oxide units. Therefore, it could be considered that no β-cyclodextrin is efficiently threaded on PEO segments.

The addition of both ring components finally leads to an interesting supramolecular fact that the cyclodextrins have to be threaded in the correct sequence. Here, statistical and energetical questions are, in principle, relevant for the quality and structure of the resulting supramolecular structure or primary sequence. It is tried now to use silica nanocasting to depict if there is a difference. The resulting data are summarized in Table 3.

For the α-MCD−block copolymer systems, only typical polyrotaxane pores are found but no larger cavities due to micelles. This means that micelle or aggregate formation of the block copolymer is effectively suppressed by the presence of α-MCD, very similar to the behavior of the much smaller nonionic surfactants. This is somewhat surprising but clearly proven by the nanocasting procedure, where the TEM images shown pore structures similar to those of the α-MCD−PEO systems.

For the block copolymer (Pluronics F-68) complexed by β-MCD, the pore structures are also similar to those of β-MCD−PPG systems. It should be emphasized that the higher porosity, even at pH 2.0, is attributable to a large amount of PEO segments, which are free and noncomplexed, because the dose amount of the copolymers is based on the ratios of PO units to β-MCD. Therefore, these results of block copolymer with β-MCD are not suitable for comparison with those with α-MCD (vide supra) and α-MCD + β-MCD (vide infra).

The simultaneous presence of α-MCD and β-MCD does give interesting results. The inclusion of a whole copolymer chain by α-MCD and β-MCD makes the porosity data different from the cases with only one cyclodextrin species. When the results at pH 3.0 are compared, it is easily found that the average pore sizes of the block copolymer with α-MCD and α-MCD + β-MCD are explicitly different, i.e., 2.89 and 4.51 nm for EOPOEO(a), respectively. The difference between the two systems is only the addition of a small amount of β-MCD in the latter case. Both the PEO and PPO segments are included for α-MCD + β-MCD systems, while the PPO segment is not included for α-MCD systems. However, the pore sizes of the block copolymer with α-MCD + β-MCD at pH 4.0 are smaller than those at pH 3.0 of the corresponding systems, which we could not explain so far.

For the block copolymer EOPOEO (Pluronics F-68), the results concerning the sequence of cyclodextrin addition are somewhat puzzling. At pH 2.0, the porosity data for systems of different sequences are very close to each other. In fact, this is valid for all investigated systems. At pH 3.0, different sequences give evidently different results. Addition of the larger β-MCD first, stirring overnight, and then addition of the smaller α-MCD [sample EOPOEO(a)] results in a larger average pore size (4.51 nm) than that (2.95 nm) of the sample EOPOEO(b) (simultaneous addition of both cyclodextrin species). For the sample EOPOEO(a), it is expected that all PPO and PEO segments are well-included into corresponding cyclodextrin cavities, while for EOPOEO-(b), it is less possible for all PPO segments to be included into β-MCD cavities. The results of sample EOPOEO-(b) are similar to those of EOPOEO−α-MCD. However, the results concerning the addition sequence at pH 4.0 are not consistent with those at pH 3.0. This means that

(42) Fujita, H.; Ooya, T.; Yui, N. *Macromolecules* **1999**, *32*, 2534−2541.

Table 3. Nitrogen Sorption Data for Porous Silicas Obtained from Cyclodextrins (α- and *β*-MCD) and PEO− and PPO−Block Containing Triblock Copolymer (Pluronics F-68) at pH 2.0, 3.0, and 4.0, Respectively

	pH 2.0			pH 3.0			pH 4.0		
	pore diameter (nm)	BET surface area (m^2/g)	pore volume (cm^3/g)	pore diameter (nm)	BET surface area (m^2/g)	pore volume (cm^3/g)	pore diameter (nm)	BET surface area (m^2/g)	pore volume (cm^3/g)
α-MCD									
EOPOEO	2.00	642	0.322	2.89	649	0.469	3.46	598	0.517
β-MCD									
EOPOEO	2.61	683	0.447	4.62	585	0.676	8.06	516	1.039
α-MCD + *β*-MCD									
EOPOEO[a]	1.96	667	0.328	4.51	591	0.667	3.66	705	0.645
EOPOEO[b]	1.99	677	0.337	2.95	662	0.520	3.70	622	0.575

[a] α-MCD was added ca. 12 h later than the addition of *β*-MCD. [b] Simultaneous addition of α-MCD and *β*-MCD.

the experiments are still not correctly designed to test if there is the possibility of a simple sequence of correctly aligned cyclodextrins onto a polymer backbone.

Conclusion

It was shown that it is possible to prove and analyze the in situ formation of pseudopolyrotaxanes between cyclodextrins and different polyethers or nonionic surfactants by silica nanocasting, i.e., by analyzing a porous solid silica replica instead of the original fragile soft matter structure.

As shown by TEM, all formed silicas at pH 2.0 possess a short tubelike pore structure with diameters of about 2.0 nm, which fits well with the expected diameter of the pseudopolyrotaxanes. In no case did we find pores due to potential micelles of the nonionic surfactants or block copolymers. Pore structures were also found to be different from pure cyclodextrin-based silica.

The pore diameter of pseudopolyrotaxane-based silica materials depends on the pH values of silica condensation, and direct replication is just obtained at pH 2.0, whereas larger pores are found at higher pH values. We interpret this as aggregation of pseudopolyrotaxanes via hydrogen bonding toward arrays or bundle structures.

The documentation of more complex binding events as the correct sequential binding of two cyclodextrins to linear block copolymers is still open. Works using other (pseudo)polyrotaxanes as the template for the nanocasting process are in progress.

Acknowledgment. We thank Wacker-Chemie AG for the donation of the methylated cyclodextrins. The help of Bernd Smarsly throughout X-ray scattering is highly appreciated. The Max-Planck Society is thanked for financial support and acknowledged by B.-H.H. for a Max Planck Society Scholarship.

CM0113088